Computers and Chemical Engineering 94 (2016) 45–59

Contents lists available at ScienceDirect

Computers and Chemical Engineering

journal homepage: www.elsevier.com/locate/compchemeng

# Probabilistic reactor design in the framework of elementary process functions

Nicolas M. Kaiser[a], Robert J. Flassig[b,*], Kai Sundmacher[a,b]

[a] Otto-von-Guericke-University Magdeburg, Department Process Systems Engineering, Universitätsplatz 2, D-39106 Magdeburg, Germany
[b] Max Planck Institute for Dynamics of Complex Technical Systems, Department Process Systems Engineering, Sandtorstr. 1, D-39106 Magdeburg, Germany

ARTICLE INFO

*Article history:*
Received 15 June 2015
Received in revised form 27 May 2016
Accepted 17 June 2016
Available online 12 July 2016

*Keywords:*
Hydroformylation
Multiphase systems
Probabilistic reactor design
Robust design optimization
Optimization under uncertainty

ABSTRACT

Computational process models in combination with innovative design methodologies provide a powerful reactor design platform. Yet, model-based design is mostly done in a pure deterministic way. Possible uncertainties of the underlying model parameters, prediction errors due to simplifying assumptions regarding the reactor behavior and suboptimal realizations of the design along the reaction coordinate are in general not considered. Here we propose a systematic design approach to directly account for the impact of such variabilities during the design procedure. The three level design approach of Peschel et al. (2010) based on the concept of elementary process functions (EPF) serves as basis. The dynamic optimizations on each level are extended within a probabilistic framework to account for different sources of randomness. The impact of these sources on the performance prediction of a design is quantified and used to robustify the reactor design aiming at a more reliable performance and thus design prediction. The uncertainties of model parameters, non-idealities of the reactor behavior and inaccuracies in the design are included via statistical moments. By means of the sigma point method (Julier and Uhlmann, 1996) random variables are mapped to the design objective space via the nonlinear process model. Importantly, this work introduces a full probabilistic orthogonal collocation approach, i.e. random and stochastic variables can be described. Whereas the former one relates to randomness independent on the reaction time (e.g. kinetic model parameters or initial conditions), the latter one describes stochasticity along the reaction time (e.g. fluctuating pressure or temperature control). As an example process the hydroformylation of 1-dodecene in a thermomorphic solvent system consisting of *n*-decane and *N*,*N*-dimethylformamide is considered.

Our probabilistic EPF approach allows designing robust optimal reactors, which operate within an estimated confidence at their expected optimum considering almost any kind of randomness arising in the design procedure. An additional value is that with increased predictive power of the reactor performance its embedding in an overall process is strongly simplified.



## 1. Introduction

A process system is composed of a variety of different units serving specific functions, to ultimately transform mass or/and energy into high-value products. Pretreatment of resources and post-processing of products are strongly depending on the requirements and the performance of the reactor unit. Computational design methodologies are used to identify and predict an optimal performing reactor design. Common reactor design methods such as heuristics or attainable region approaches (Glasser et al., 1987; Horn, 1964) yield only solutions, which are limited by the set of predefined reactors and are not very practical for higher-dimensional systems. Mostly they do not consider the requirements for complex reaction networks, behavior of complex solvent systems and recycles. Freund and Sundmacher (2008) have developed a design approach, which is not based on predefined reactor types. It is fully decoupled from the limitations of certain apparatuses so that the full thermodynamical and chemical potential of the process can be explored leading to new integrated reactor concepts. Several examples for the application of the concept of elementary process functions (EPF) toward a deterministic design of optimal reactors have recently been presented by Freund et al. (2011) and Peschel et al. (2011). State-of-the-art reactor design methodologies typically involve computational intense optimizations of superstructures (Achenie and Biegler, 1990; Kokossis and Floudas, 1991)

* Corresponding author.
*E-mail address:* flassig@mpi-magdeburg.mpg.de (R.J. Flassig).

http://dx.doi.org/10.1016/j.compchemeng.2016.06.008
0098-1354/

**Nomenclature**

*Latin symbols*

| | |
|---|---|
| $a_i$ | coefficients for Gibbs energy equations [diverse, see Table 2] |
| $a_\rho$ | coefficients for density equations |
| $c$ | concentration [mol/ml] |
| $Cov$ | covariance matrix |
| $D$ | design |
| d$t$ | differential time |
| $E$ | mean value of variable/parameter |
| $E_A$ | activation energy [kJ/mol] |
| f | right-hand side function of the ODE within the collocation |
| $f, g, h$ | nonlinear functions |
| $G$ | Gibbs energy [kJ/mol] |
| g | equality constraints |
| h | inequality constraints |
| $H_i$ | Henry coefficient for component $i$ |
| $H_i^0$ | Henry parameter for component $i$ [bar ml/mol] |
| $i, j, k, l, m$ | index |
| iso | branched form of component |
| j | molar flux [mol/min] or arbitrary flux [(. . .)/min] |
| $k_0$ | reaction rate constant [diverse, see Table 1] |
| $M$ | molar mass [g/mol] |
| $n$ | amount of substance [mol], or number of parameters in a set, or linear form of component |
| $O$ | arbitrary criterion |
| $o$ | realization of an arbitrary criterion |
| $p$ | parameter |
| $p_i$ | partial pressure [bar] |
| $q$ | heat flux [J/min] |
| $R$ | gas constant [kJ/mol/K] |
| $r_j$ | reaction rate [mol/g/min] |
| $S$ | selectivity |
| $s$ | realization of selectivity |
| $T$ | temperature and realization of $T$ [K] |
| $t$ | time [min] |
| $\boldsymbol{u}$ | control variable |
| $V$ | volume [ml] |
| $Var$ | variance of a variable/parameter |
| $W$ | weighting matrix |
| $w$ | work [J] |
| $X$ | conversion |
| $x$ | arbitrary state variable, or realization of $X$ |

*Abbreviations*

| | |
|---|---|
| CO | carbon monoxide |
| $CO_2$ | carbon dioxide |
| COM | set of liquid reactants |
| CSTR | continuous stirred tank reactor |
| DAE | differential algebraic equation |
| DDO | deterministic dynamic optimization |
| DDOP | deterministic dynamic optimization problem |
| DMF | dimethyl formamide |
| DOE | design of experiments |
| DOP | dynamic optimization problem |
| EPF | elementary process functions |
| ***EPF*** | matrix of elementary process functions |
| FE | finite elements |
| GMD | Gaussian mixed distributions |
| $H_2$ | hydrogen |
| MDOP | methodical dynamic optimization problem |
| MOO | multi-objective optimization |
| ODE | ordinary differential equation |
| PDE | partial differential equation |
| PDOP | probabilistic dynamic optimization problem |
| RBDO | reliability-based design optimization |
| RCT | set of reactions |
| RDO | robust design optimization |
| RTD | residence time distribution |
| STY | space time yield |
| TMS | thermomorphic solvent |
| WS | method of weighted sum |
| $\varepsilon$-CM | $\varepsilon$-constraint method |
| nC12en | 1-dodecene |
| iC12en | iso-dodecenes |
| nC12an | *n*-dodecane |
| nC13al | *n*-tridecanal |
| iC13al | isomeric aldehyde |
| nC10an | *n*-decane |

*Greek symbols*

| | |
|---|---|
| $\alpha, \kappa, \beta, \lambda$ | tuning factor for sigma point method |
| $\Delta$ | difference |
| $\varepsilon$ | parameter deviation |
| $\Theta, \theta$ | random variable, or uncertain model parameters |
| $\rho$ | density function |
| $\rho_i$ | density of component $i$ [g/ml] |
| $\sigma$ | source term [mol/min], or variance |
| $\tau$ | residence time [min] |

*Indices*

| | |
|---|---|
| A | areal |
| c | collocation points |
| cat | catalyst |
| max | maximum value |
| min | minimum value |
| ref | reference value |
| t | technical |
| tot | total amount |
| V | volumetric |
| $\alpha$ | arbitrary component(s) |
| $\Theta$ | set of random variables, or uncertain model parameters |
| **Bold font** | vector-valued variable |

or dynamic optimization problems (see e.g. Hillestad, 2010; Peschel et al., 2010; Srinivasan et al., 2003a,b).

For any design methodology it is of vital importance to have reliable and accurate model predictions to reduce or even avoid costly redesign, process sensors and controller equipment. However, the predictive power of mathematical models regarding the reactor performance can be limited. The limitation originates from different kinds of assumptions within common design procedures, e.g. fixed model parameters, simplifications regarding reactor behavior (=non-idealities) or perfect realization of the resulting process design. In a deterministic design procedure these limitations are completely ignored. To quantify the impacts of neglected model parameter uncertainties, non-ideal reactor behavior and design inaccuracies (see e.g. Beyer and Sendhoff, 2007) their random character must be incorporated into the design optimization. This can be done by use of probabilistic-based design procedures.

Two different approaches can be found in literature: reliability-based design optimization (RBDO) and robust design optimization (RDO) (see e.g. Schuëller and Jensen, 2008). Reliability-based design optimization aims at ensuring a specified reliability of the

performance, i.e. the design is supposed to violate certain prescribed probabilistic constraints such as probabilities of failure or reliability indices only with an acceptable likelihood. The solution provides an optimal design at given confidence with respect to its reliability (see e.g. Enevoldsen and Sørensen, 1994; Li et al., 2008). In contrast, robust design optimization aims at maximizing the performance of the process by minimizing the sensitivity of the objective function(s) to different sources of randomness. It is typically applied to robustify the process against uncertainties by optimal choice of the control or design variables for fixed constraints (see e.g. Beyer and Sendhoff, 2007; Mulvey and Vanderbei, 1995). Notably, existing probabilistic reactor design approaches do not handle stochastic variables, i.e. fluctuations along the reaction coordinate. Such fluctuations are however very likely to be found in the real process and include fluctuations in the optimal design itself. Note however that stochastic variabilities are non-trivial to embed into a reactor design procedure as this results in a stochastic ODE/DAE or PDE system with heavily increased computational burden.

In this work we present a probabilistic design methodology that handles random and stochastic variables in ODE/DAE systems. We use orthogonal collocation on finite elements (see e.g. Biegler, 1983) in combination with the sigma point methodology by Julier and Uhlmann (1996) to derive a discretized numeric probabilistic representation. The presented probabilistic orthogonal collocation approach provides the basis for reactor design approaches that rely on dynamic optimization or optimal control problem formulations. Here we focus on the structured EPF reactor design approach to highlight different sources of randomness that can be accounted for during the design procedure to ultimately obtain a reliably performing optimal reactor.

In the following section the conceptual basis of the EPF reactor design procedure including a 3-level structure, the mathematical basis of the sigma point method and its use for RDO in the form of a discretized optimal control problem is introduced. Subsequently the model of the hydroformylation process is shown and the different types of random and stochastic variabilities are included in the EPF design approach. Section 3 covers the results of the RDO in each level of the reactor design approach for the aforementioned example process. The article closes with a discussion in Section 4 and conclusion in Section 5.

## 2. Methods

### 2.1. Process design via elementary process functions

In the EPF approach a fluid element is tracked along the reaction coordinate while its thermodynamic states are optimized by manipulating external mass and energy fluxes, see Fig. 1. Along the chemical reaction coordinate the composition of the fluid element experiences a continuous change, which can be adjusted by the external fluxes ($j_{\alpha,A}$, $q_A$, $w_t$) to reach a desired state configuration at the end of the reaction process.

Based on the EPF concept, Peschel et al. (2010) developed a three level reactor design procedure. On level 1, the maximum potential of the process is revealed for different enhancement concepts resulting in optimal mass and energy fluxes into/out of the fluid element. In each enhancement concept different constant and variable fluxes are considered in the dynamic optimization. In a second step (level 2) limitations due to transport kinetics describing physical phenomena are considered and control variables are chosen to realize the optimal mass and energy fluxes from level 1. In the third level the trajectories of the control variables are then realized in an optimal but non-unique technical approximation to obtain the final reactor design. So far the EPF based reactor design procedure assumes model parameters as perfectly determined. Furthermore the reactor behavior is partly idealized regarding e.g. pressure drop, flow field or temperature gradients when transforming the problem from the time-based optimal control to a continuous design. The possible inaccuracies in the technical approximation, by e.g. actuator or controller imprecisions or variations in the feed, are also not taken into account. In a probabilistic interpretation, randomness resulting from uncertainties in model parameters, non-idealities in the reactor characteristics or inaccuracies in the reactor design can be represented by an appropriate density distribution function. The challenge lies then in efficiently describing how the density functions are transformed by the nonlinear process model and thus mapped to the space of design objectives, see Fig. 2.


**Fig. 1.** Fluid element with control fluxes, $j_{\alpha,A}$ – surface related dosing fluxes of components $\alpha$, $q_A$ – surface related heat flux, $w_t$ – technical work, $r_{\alpha,V}$ – volume related source/sink term of components $\alpha$.

### 2.2. Sigma point method

A very efficient and accurate method for nonlinear transformation of random variables is the sigma point method (Julier and Uhlmann, 1996). It has been successfully applied in several challenging applications including design of experiments (DOE) (see e.g. Flassig and Sundmacher, 2012; Schenkendorf et al., 2009; Telen et al., 2014), the design of robust optimal process trajectories (see e.g. Rossner et al., 2010) and for the design of robust model predictive controller (see e.g. Heine et al., 2006).

The idea of the sigma point method is to describe how mean $E(\boldsymbol{\theta})$ and covariance $Cov(\boldsymbol{\theta})$ of a density function $\rho_{\boldsymbol{\Theta}}(\boldsymbol{\theta})$ of an $n_{\boldsymbol{\theta}}$ – dimensional random variable $T_{ref} = 378.15\,K$ are transformed by a nonlinear mapping $\mathbf{h} : \mathbb{R}^{n_{\boldsymbol{\theta}}} \rightarrow \mathbb{R}^{n_{\mathbf{h}}}$. The distribution $\rho_{\boldsymbol{\Theta}}(\boldsymbol{\theta})$ characterized by $E(\boldsymbol{\theta})$ and $Cov(\boldsymbol{\theta})$ is approximated via $2n_{\boldsymbol{\theta}} + 1$ sigma points given by

$$\boldsymbol{\theta}_0 = E(\boldsymbol{\theta}), \tag{1}$$

$$\boldsymbol{\theta}_i = \boldsymbol{\theta}_0 + \mathrm{sign}(n_{\boldsymbol{\theta}} - i)\sqrt{(n+\kappa)}\sqrt{Cov(\boldsymbol{\theta})}_i, \quad i = 1\ldots 2n_{\boldsymbol{\theta}}, \tag{2}$$

where $\sqrt{Cov(\boldsymbol{\theta})}_i$ is the $i$th row or column of the matrix square root of $Cov(\boldsymbol{\theta})$ and sign the signum function. The sigma points $\boldsymbol{\theta}_i$ with $i = 0, 1\ldots, 2n_{\boldsymbol{\theta}}$ are transformed via the nonlinear transformation $\mathbf{h}(\boldsymbol{\theta}_i) = \mathbf{o}_i$ to yield the set of transformed sigma points in the range $\mathbb{R}^{n_{\mathbf{h}}=n_{\mathbf{o}}}$ of $\mathbf{h}$. With this set, mean and covariance in the range of $\mathbf{h}$ can be calculated via

$$E(\mathbf{o}) = \sum_{i=0}^{2n} w_i \mathbf{o}_i \tag{3}$$

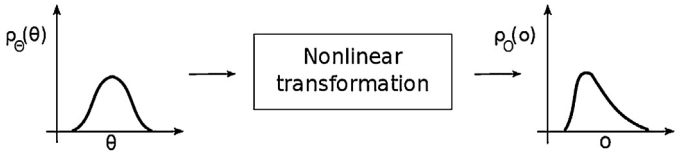


**Fig. 2.** Propagation of random variables via nonlinear transformation, $\rho$ – density function, $\Theta$ – set of random.

$$Cov(\mathbf{o}) = \sum_{i=0}^{2n} w_i \left\{\mathbf{o}_i - E(\mathbf{o})\right\} \left\{\mathbf{o}_i - E(\mathbf{o})\right\}^{\mathrm{T}}. \quad (4)$$

The weighting factors are

$$w_0 = \frac{\lambda}{n_{\boldsymbol{\theta}} + \lambda}, \quad w_i = \frac{\lambda}{2(n_{\boldsymbol{\theta}} + \lambda)}, \quad i = 1, \ldots 2n_{\boldsymbol{\theta}} \quad (5)$$

The tuning parameter $\lambda$, with $\lambda \in \mathbb{R}$, for higher order moments is calculated via $\lambda = \alpha^2(n_{\boldsymbol{\theta}} + \kappa) - n_{\boldsymbol{\theta}}$. For selecting the tuning parameters $\alpha$, $\beta$ and $\kappa$, Julier et al. (2000) suggest some rule of thumbs depending on the knowledge of the parameter distribution functions of the random variables. We used $\kappa = 1$.

In the EPF concept, the nonlinear transformation $\mathbf{h}\left(\boldsymbol{\theta}, D\right) = \mathbf{g}\left(\mathbf{f}\left(\boldsymbol{\theta}, D\right)\right)$ can be decomposed into a function $\mathbf{f}$ that maps uncertain variables onto the model states, and a function $\mathbf{g}$, which maps the process state variables onto the space of design objectives. By changing the reactor design $D$, the nonlinear transformation $\mathbf{O} = \mathbf{h}(\boldsymbol{\theta}, D)$ is varied. In case of a single objective robust design optimization the aim is to identify a design $D$ that has a very small variance $Var(o|D)$ of the best-expected objective $E(o|D)$. Then the expected objective is insensitive with respect to the uncertain variables. The use of the sigma point for RDO purposes is illustrated in Fig. 3.

### 2.3. Dynamic optimization: probabilistic orthogonal collocation

The EPF method was introduced as conceptual basis of the reactor design approach, where the applied model class is a DAE system. The DAE system consists of ODEs of the balance equations, which are formulated in the Lagrangian formalism and algebraic equations for phase properties, reaction kinetics and physical boundaries. The manipulating fluxes are the solutions of dynamic optimizations, which are constrained by the DAE system. In this work orthogonal collocation on finite elements method is used (Biegler, 1983), to solve the standard deterministic dynamic optimization problem of the EPF framework (Freund and Sundmacher, 2008). The problem reads

$$\text{opt}_{\mathbf{u}(t),\mathbf{p}}\ \mathbf{o} \qquad \text{(MDOP 1)}$$

$$\text{s.t.} \quad \frac{\mathrm{d}\mathbf{x}}{\mathrm{d}t} = \mathbf{EPF}(\mathbf{x})\mathbf{j}(t) + \boldsymbol{\sigma}(\mathbf{x}) \equiv \mathbf{f}(\mathbf{x}(t), \boldsymbol{\theta}, \mathbf{u}(t), \mathbf{p})$$

(Material, energy balances),

$$\mathbf{h}(\mathbf{x}) = 0 \,(\text{Kinetics, physical properties, etc.}),$$

$$\mathbf{g}(\mathbf{x}) \geq 0 \,(\text{Boundaries, solubilities, etc.})$$

where, $\mathbf{o}$ is the objective to be optimized by adjusting the control variables $\mathbf{u}(t)$ and design parameters $\mathbf{p}$, e.g. dimensions of the reactor, and $\boldsymbol{\theta}$ are model parameters. The differential equations, typically material and energy balances, are consisting of the elementary process function matrix $\mathbf{EPF}(\mathbf{x})$, the fluxes $\mathbf{j}(t)$ and a source/sink term $\boldsymbol{\sigma}(\mathbf{x})$. With orthogonal collocation, the resulting NLP problem reads

$$\text{opt}_{\mathbf{u}_{l=1\ldots nFE},\mathbf{p}}\ \mathbf{o} \qquad \text{(MDOP 2)}$$

$$\text{s.t.} \quad \mathbf{x}_{lk} = \mathbf{x}_{l0} + \mathrm{d}t_l \sum_{j=0}^{n_{\mathrm{CP}}-1} \mathbf{W}_{kj}\mathbf{f}(\mathbf{x}_{lj}, \boldsymbol{\theta}, \mathbf{u}_l, \mathbf{p}) \quad \forall l = 1, \ldots, n_{\mathrm{FE}},$$

$$\forall k = 1, \ldots, n_{\mathrm{CP}}$$

$$\mathbf{x}_{l-1,n_{\mathrm{CP}}-1} = \mathbf{x}_{l0} \quad \forall l = 2, \ldots, n_{\mathrm{FE}}$$

$$\mathbf{x}_{l0} = \mathbf{x}_0$$

$$+ \text{additional constraints } \mathbf{h}(\mathbf{x}) = 0 \quad \text{and } \mathbf{g}(\mathbf{x}) \geq 0 \quad \text{in discretized form}$$

Here, $n_{\mathrm{CP}}$ represents the number of collocation points on each finite element $l = 1, \ldots, n_{\mathrm{FE}}$ and $\mathbf{W}_{kj}$ the collocation point weighting matrix. The control $\mathbf{u}(t)$ is discretized as piecewise constant on each finite element.

#### 2.3.1. Random variables

To account for random variables such as $n_{\boldsymbol{\theta}}$ uncertain model parameters (including kinetic model parameters and initial conditions) in level 1 of the design approach, the NLP is enlarged by a factor of $2n_{\boldsymbol{\theta}}$ when applying the sigma point approach. The resulting NLP problem reads

$$\left.\begin{aligned}
&\text{opt}_{\mathbf{u}1=1,\ldots,n_{\mathrm{FE}'},\mathbf{p}}\ [E(\mathbf{O}),\ Cov(\mathbf{O})]^{\mathbf{T}} \qquad \text{(MDOP 3)}\\
&\text{s.t.} \quad \mathbf{x}_{ilk} = \mathbf{x}_{il0} + \mathrm{d}t_{il} \sum_{j=0}^{n_{\mathrm{CP}}-1} \mathbf{W}_{kj}\mathbf{f}(\mathbf{x}_{ilj}, \theta_i, \mathbf{u}_l, \mathbf{p}) \quad \forall l = 1, \ldots, n_{\mathrm{FE}}, \quad \forall k = 1, \ldots, n_{\mathrm{CP}}\\
&\mathbf{x}_{i,l-1,n_{\mathrm{CP}-1}} = \mathbf{x}_{ilo} \quad \forall l = 2, \ldots, n_{\mathrm{FE}}\\
&\mathbf{x}_{i10} = \mathbf{x}_{i0}\\
&\mathrm{d}t_{il} = \frac{\tau_i}{n_{\mathrm{FE}}} \quad \forall l = 1, \ldots, n_{\mathrm{FE}}\\
&+ \text{additional constraints } \mathbf{h}(\mathbf{x}) = 0 \quad \text{and } \mathbf{g}(\mathbf{x}) \geq 0 \quad \text{in discretized form for } i, l, k
\end{aligned}\right\} \quad \forall i = 0, \ldots, 2n_{\boldsymbol{\theta}}$$

$$\mathbf{o}_i = \mathbf{h}(\mathbf{x}_{ilk}) \quad \forall l = 1, \ldots, n_{\mathrm{FE}}, \quad k = 0, \ldots, (n_{\mathrm{CP}} - 1)$$

$$E(\mathbf{o}) = \sum_{i=0}^{2n_{\boldsymbol{\theta}}} w_i \mathbf{o}_i$$

$$Cov(\mathbf{o}) = \sum_{i=1}^{2n_{\boldsymbol{\theta}}} w_i \{\mathbf{o}_i - E(\mathbf{o})\}\{\mathbf{o}_i - E(\mathbf{o})\}^{\mathrm{T}}.$$

In level 2 non-ideal reactor characteristics are included as random variables $\vartheta$ as well to the design approach. The aforementioned discretized optimization problem is hence extended to

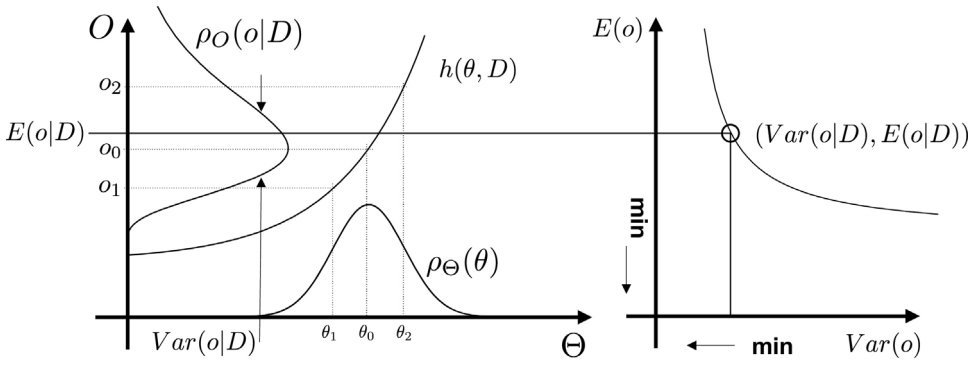


**Fig. 3.** Left: Sigma point mapping from the parameter space Θ to the criterion space O by the process model h depending on the chosen design *D*. Right: Corresponding design point in a Pareto set.

$$
\begin{aligned}
&\text{opt}_{\mathbf{u}_{l=1,\ldots,n_{\text{FE}}},\mathbf{p}} \quad [E(\mathbf{o}), Cov(\mathbf{o})]^{\text{T}} \qquad \text{(MDOP 4)} \\
&\text{s.t.} \quad \mathbf{x}_{imlk} = \mathbf{x}_{iml0} + \mathrm{d}t_{il} \sum_{j=0}^{n_{\text{CP}}-1} \mathbf{W}_{kj} \mathbf{f}(\mathbf{x}_{imlj}, \boldsymbol{\theta}_i, \boldsymbol{\vartheta}_m, \mathbf{u}_l, \mathbf{p}) \quad \forall l = 1, \ldots, n_{\text{FE}}, \quad \forall k = 1, \ldots, n_{\text{CP}} \\
&\quad \mathbf{x}_{i,m,l-1,n_{\text{CP}}-1} = \mathbf{x}_{iml0} \quad \forall l = 2, \ldots, n_{\text{FE}} \\
&\quad \mathbf{x}_{im10} = \mathbf{x}_{im0} \\
&\quad \mathrm{d}t_{il} = \frac{\tau_i}{n_{\text{FE}}} \quad \forall l = 1, \ldots, n_{\text{FE}} \\
&\quad + \text{additional constraints } \mathbf{h}(\mathbf{x}) = 0 \text{ and } \mathbf{g}(\mathbf{x}) \geq 0 \quad \text{in discretized form for } i, m, l, k
\end{aligned}
\Bigg\} \quad \forall i = 0, \ldots, 2n_{\boldsymbol{\theta}}, \quad \forall m = 0, \ldots, 2n_{\boldsymbol{\vartheta}}
$$

$$
\begin{aligned}
&\mathbf{o}_{im} = \mathbf{h}(\mathbf{x}_{imlk}) \quad \forall l = 1, \ldots, n_{\text{FE}}, \quad k = 0, \ldots, (n_{\text{CP}} - 1) \\
&E(\mathbf{o}) = \sum_{m=0}^{2n_{\boldsymbol{\vartheta}}} \left( \mathrm{w}_m \sum_{i=0}^{2n_{\boldsymbol{\theta}}} \mathrm{w}_i \mathbf{o}_{im} \right) \\
&Cov(\mathbf{o}) = \sum_{m=0}^{2n_{\boldsymbol{\vartheta}}} \left( \mathrm{w}_m \left( \sum_{i=0}^{2n_{\boldsymbol{\theta}}} \mathrm{w}_i \{\mathbf{o}_{im} - E(\mathbf{o})\} \{\mathbf{o}_{im} - E(\mathbf{o})\}^{\text{T}} \right) \right).
\end{aligned}
$$

#### 2.3.2. Stochastic variables

To account for stochastic variables, e.g. reaction coordinate dependent randomness from fluctuations of the optimal control variable $\mathbf{u}(t)$, we propose the following discretization:

$$
\begin{aligned}
&\text{opt}_{\mathrm{E}_{l=1,\ldots,n_{\text{FE}}}(\mathbf{u}_l),\mathbf{p}} \, \mathbf{o} \qquad \text{(MDOP 5)} \\
&\text{s.t.} \quad \mathbf{x}_{ilk} = E_{\mathbf{u}_l}(\mathbf{x}_{l0}) + \mathrm{d}t_l \sum_{j=0}^{n_{\text{CP}}-1} \mathbf{W}_{kj} \mathbf{f}(E_{\mathbf{u}_l}(\mathbf{x}_{lj}), \boldsymbol{\theta}, \boldsymbol{\vartheta}, \mathbf{u}_{il}, p) \quad \forall l = 1, \ldots, n_{\text{FE}}, \quad \forall k = 1, \ldots, n_{\text{CP}} \\
&\quad E_{\mathbf{u}_{l-1}}(\mathbf{x}_{l-1,n_{\text{CP}}-1}) = E_{\mathbf{u}_l}(\mathbf{x}_{l0}) \quad \forall l = 2, \ldots, n_{\text{FE}} \\
&\quad \mathbf{x}_{i10} = E_{\mathbf{u}_l}(\mathbf{x}_{i0}) \\
&\quad + \text{additional constraints } \mathbf{h}(\mathbf{x}) = 0 \text{ and } \mathbf{g}(\mathbf{x}) \geq 0 \text{ in discretized form for } i, l, k
\end{aligned}
\Bigg\} \quad \forall i = 0, \ldots, 2n_{\mathbf{u}}
$$

$$
\begin{aligned}
&E_{\mathbf{u}_l}(\mathbf{x}_{lk}) = \sum_{i=0}^{2n_{\mathbf{u}}} \mathrm{w}_i \mathbf{x}_{ilk} \quad \forall l = 1, \ldots, n_{\text{FE}}, \quad k = 0, \ldots, (n_{\text{CP}} - 1) \\
&\mathbf{o} = \mathbf{h}\left(E_{\mathbf{u}_l}(\mathbf{x}_{lk})\right) \quad \forall l = 1, \ldots, n_{\text{FE}}, \quad k = 0, \ldots, (n_{\text{CP}} - 1),
\end{aligned}
$$

where the reaction coordinate dependent fluctuating variable is transformed on each finite element l via the sigma point method given $E_l(\mathbf{u}_l)$ and $Cov(\mathbf{u})$. Note that here the mean of the control variable for given variance–covariance is optimized.

### 2.4. Multi-objective design optimization

Even for a single-objective design optimization, the extension to a probabilistic design approach leads to a multi-objective optimization (MOO) problem, since expected value *E*(o) and variance *Var*(o) are to be optimized. In this case we deal with a set of Pareto optimal solutions from which a design can be chosen given a specific trade-off between expected objective *E*(o) and its variance *Var*(o) (= predictive power). An excellent review on multi-objective optimization problems in the field of process design can for instance be found in Bhaskar et al. (2000). The existing approaches for identifying the Pareto optimal solutions can be separated into *vectorial* methods and *scalar* methods. In the former case, the MOO is directly solved with a vector-valued objective function, whereas in the latter case several objectives are transformed into a scalar function. For the sake of brevity the different methods will not be discussed. Details can be found e.g. in Marler and Arora (2004). In the present work the *Method of Weighted Sum* (WS) and the *ε-constraint Method* (ε-CM) are used.

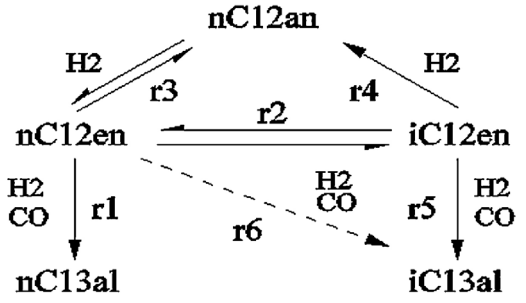


**Fig. 4.** Extended reaction network of the rhodium catalyzed hydroformylation in TMS as derived in Hentschel et al. (2015). nC12en = 1-dodecene, iC12en = internal dodecenes, nC12an = *n*-dodecane, nC13al = *n*-tridecanal, and iC13al = internal aldehydes.

The WS is used to find reasonable ranges of the two objectives, where Pareto optimal solutions might exist. Then within this ranges the Pareto set is calculated via the $\varepsilon$-CM.

### 2.5. Example process

The robust design optimization framework developed here is applied on the hydroformylation process of long-chained alkenes. The alkenes are functionalized via addition of CO and $H_2$ to aldehydes which are used as platform chemicals for many applications. The reaction is homogeneously catalyzed by rhodium catalysts and the selectivity to the desired linear aldehyde is increased by use of expensive biphephos ligands. For the sake of economic viability the catalyst and ligand have to be separated and recycled almost completely (Xie et al., 2013). The arising aldehydes are produced as a mixture of linear (n) and branched (iso) forms, whereby the demand for linear aldehydes is much higher. More information about hydroformylation processes can be found in e.g. Wiebus and Cornils (1994) and Bohnen and Cornils (2002).

The industrial most relevant process for rhodium catalyzed hydroformylation is the Ruhrchemie-Rhône/Poulenc process (see e.g. Kohlpaintner et al., 2001). This process is not applicable for long-chained alkenes (>C4) due to low solubility of reactants in the process solvent. To overcome both the problem of solubility of the reactants and the problem of separation and recycling of expensive catalyst in the hydroformylation process of long-chained alkenes, several innovative solvent systems are under investigation. Among others, thermomorphic solvent (TMS) systems (see e.g. Behr and Fängewisch, 2002; Behr et al., 2008) show promising performance for hydroformylation of long-chained alkenes. Therefore a TMS system according to Schäfer et al. (2012) consisting of *N*,*N*-dimethylformamide (DMF) as polar solvent and *n*-decane as nonpolar solvent is assumed in this work for reactor design purposes.

### 2.6. Model formulation

For the special TMS system of *n*-decane and dimethylformamide Markert et al. (2013) and Kiedorf et al. (2014) investigated experimentally the hydroformylation of 1-dodecene catalyzed by the rhodium(acac)($CO_2$)/biphephos catalyst and derived a reaction network and the related rate expressions, respectively. In a subsequent work Hentschel et al. (2015) refined the kinetic background of this process resulting in an extended reaction network shown in Fig. 4. They also refined rate equations (6)–(11). Besides the chemical reaction rates there is a kind of catalyst equilibrium previous to the catalytic cycles, shown in Eq. (12). The reaction network consists of 6 competing reactions, namely the hydroformylation of 1-dodecene to the desired main product *n*-tridecanal ($r_1$), the reversible isomerization of 1-dodecene ($r_2$) and its hydrogenation to *n*-decane ($r_3$), the hydrogenation of the internal dodecenes ($r_4$), the hydroformylation of the internal dodecenes ($r_5$) and the hydroformylation of the main educt 1-dodecene to the internal aldehyde ($r_6$). Latter reaction was added by refinement of the reaction network.

$$r_1 = \frac{k_{1,0}(T)\, c_{\mathrm{nC12en}} c_{\mathrm{H2}} c_{\mathrm{CO}}}{1 + K_{1,1} c_{\mathrm{nC12en}} + K_{1,2} c_{\mathrm{nC13al}} + K_{1,3} c_{\mathrm{H2}}} \tag{6}$$

$$r_2 = \frac{k_{2,0}(T)\left(c_{\mathrm{nC12en}} - \frac{c_{\mathrm{iC12en}}}{K_{\mathrm{p},2}}\right)}{1 + K_{2,1} c_{\mathrm{nC12en}} + K_{2,2} c_{\mathrm{iC12en}}} \tag{7}$$

$$r_3 = \frac{k_{3,0}(T)\left(c_{\mathrm{nC12en}} c_{\mathrm{H2}} - \frac{c_{\mathrm{nC12an}}}{K_{\mathrm{p},3}}\right)}{1 + K_{3,1} c_{\mathrm{nC12en}} + K_{3,2} c_{\mathrm{nC12an}} + K_{3,3} c_{\mathrm{H2}}} \tag{8}$$

$$r_4 = k_{4,0}(T)\, c_{\mathrm{iC12en}} c_{\mathrm{H2}} \tag{9}$$

$$r_5 = k_{5,0}(T)\, c_{\mathrm{iC12en}} c_{\mathrm{H2}} c_{\mathrm{CO}} \tag{10}$$

$$r_6 = k_{6,0}(T) c_{\mathrm{nC12en}} c_{\mathrm{H2}} c_{\mathrm{CO}} \tag{11}$$

$$c_{\mathrm{cat}} = \frac{c_{\mathrm{cat,tot}}}{1 + K_{\mathrm{cat},1} c_{\mathrm{CO}}^{K_{\mathrm{cat},3}} + K_{\mathrm{cat},2} \frac{c_{\mathrm{CO}}^{K_{\mathrm{cat},3}}}{c_{\mathrm{H2}}}} \tag{12}$$

The temperature dependencies of the reaction constants $k_{j,0}$ are modeled via an Arrhenius equation, with $T_{\mathrm{ref}} = 378.15\,\mathrm{K}$

$$k_j(T) = k_{0,j} \exp\left(\frac{-E_{A,j}}{R}\left(\frac{1}{T} - \frac{1}{T_{\mathrm{ref}}}\right)\right), \quad j \in RCT \tag{13}$$

The equilibrium constants $K_{p,j}$ are calculated via

$$K_{p,j} = \exp\left(\frac{-\Delta G_j}{RT}\right), \tag{14}$$

$$\Delta G_j = a_{0,j} + a_{1,j} T + a_{2,j} T^2, \quad j \in \{2, 3\}. \tag{15}$$

The parameters for rate equations and reaction constants are given in Tables 1 and 2.

Although the process consists of a liquid and gas phase only the former one is modeled and the latter is treated as a service phase, which can be manipulated by adjusting its partial pressures (Hentschel et al., 2014). The material balance for the liquid phase components (COM) in Eq. (16) consists only of the source term containing the reaction rates weighted with the catalyst mass

$$\frac{\mathrm{d}n_i^{\mathrm{liq}}}{\mathrm{d}t} = c_{\mathrm{cat}} M_{\mathrm{cat}} V_{\mathrm{liq}} \sum\nolimits_{j \in R} \nu_{i,j} r_j, \quad i \in COM. \tag{16}$$

Ideal mixing is assumed for the phase within the fluid element and thus there are no gradients inside.

The volume of the liquid phase is determined in Eq. (17), the required densities are given via Eq. (18)

$$V_{\mathrm{liq}} = \sum_{i \in \mathrm{COM}} \frac{n_i^{\mathrm{liq}} M_i}{\rho_i}, \tag{17}$$

$$\rho_i = a_{\rho,0,i} + a_{\rho,1,i} T. \tag{18}$$

The corresponding parameters can be found in Table S1.

The concentrations of the dissolved gases in the liquid phase are equal to their maximal solubilities, which are calculated with their partial pressures and Henry coefficients expressed with an exponential expression for the temperature dependency

$$c_i^* = \frac{p_i}{H_i}, \quad i \in \{GAS\}, \tag{19}$$

$$H_i = H_i^0 \exp\left(\frac{-E_{A,H_i}}{RT}\right), \tag{20}$$

**Table 1**
Parameters for rate equations and catalyst equilibrium (Eqs. (6)–(14)).

| Variable | Eq. | $E_A$ (kJ/mol) | $k_0$ | Unit | $K_1$ (ml/mol) | $K_2$ (ml/mol) | $K_3$ (ml/mol) |
|---|---|---|---|---|---|---|---|
| $r_1$ | (1) | 113.08 | 4.904e16 | $\frac{ml^3}{g\ min\ mol^2}$ | 574,876 | 3,020,413 | 11,732,838 |
| $r_2$ | (2) | 136.89 | 4.878e6 | $\frac{ml}{g\ min}$ | 38,632 | 223,214 | – |
| $r_3$ | (3) | 76.11 | 2.724e8 | $\frac{ml^2}{g\,min\,mol}$ | 2661.2 | 7100 | 1280 |
| $r_4$ | (4) | 102.26 | 2.958e4 | $\frac{ml^2}{g\,min\,mol}$ | – | – | – |
| $r_5$ | (5) | 120.84 | 3.702e10 | $\frac{ml^3}{g\ min\ mol^2}$ | – | – | – |
| $r_6$ | (6) | 113.08 | 3.951e11 | $\frac{ml^3}{g\ min\ mol^2}$ | – | – | – |
| $c_{cat}$ | (7) | – | – | – | 3.041e4 | 0 | 0.644 |

**Table 2**
Parameters for equilibrium constants (Eq. (15)).

| Variable | $a_0$ (kJ/mol) | $a_1$ (kJ/mol K) | $a_2$ (kJ/mol K$^2$) |
|---|---|---|---|
| $\Delta G_2$ | −11.0034 | 0 | 0 |
| $\Delta G_3$ | −126.275 | 0.1266 | 6.803e−6 |

**Table 3**
Parameters for the solubility coefficient calculation in Eq. (20).

| Component | $H_0$ (bar ml/mol) | $E_{A,H}$ (kJ/mol) |
|---|---|---|
| $H_2$ | 66,400 | −3.06 |
| CO | 73,900 | −0.84 |

with refined parameters of the Henry coefficient equations, see Table 3.

### 2.7. EPF based design

In the following the inclusion of the aforementioned sources of randomness for each level and the corresponding modifications of the dynamic optimization problem (DOP) in each level owing the inclusion of random variables are described. Since the reactor performance is characterized not only by the selectivity to the desired product, additional performance measures have to be considered, including space-time yield (STY), conversion and regio-selectivity. Although they are not subject of the optimization, they ought to be as high as possible. Thus, they are forced to stay in reasonable bounds during the optimization. The space-time yield is constrained by a reference STY of a continuous stirred tank reactor (CSTR) at 80% conversion. In an industrial adaptation of this process under the same conditions this seems to be a reasonable reference process. The regio-selectivity ($n$/iso ratio) is supposed to stay higher than 95% to ensure that the complexity of the subsequent separation process is not too high.

#### 2.7.1. Level 1 optimization

In level 1 the main objective is to explore the maximum potential of the process by investigating the reaction network without any transport kinetic limitations. The only boundaries to account for are intrinsic properties of the catalyst system. Owing to its intention, level 1 seems to be the ideal step to take model parameter uncertainties into account, which are entering the model as uncertain model information (see Fig. 5), e.g. parameters of the underlying reaction rate system or gas solubilities. Model parameter uncertainties result from experiments and the subsequent parameter estimations, which are done partly in Kiedorf et al. (2014) and Hentschel et al. (2015). For some of the model parameters no reference for uncertainties is available and therefore typically arising uncertainties are assumed. The nominal values of the model parameters in the deterministic optimization are given in Tables 1–3 and the confidence intervals of them used in the robust

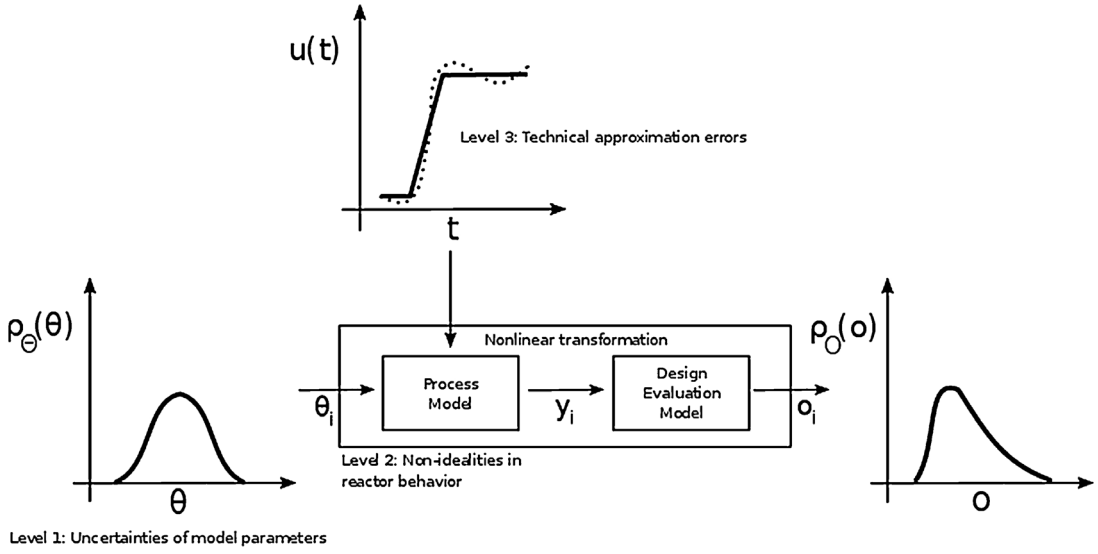


**Fig. 5.** Introduction of types of uncertainties in optimization environment, index $i$ – sigma points, $y$ – output of the process model, $o$ – output of the design evaluation model.

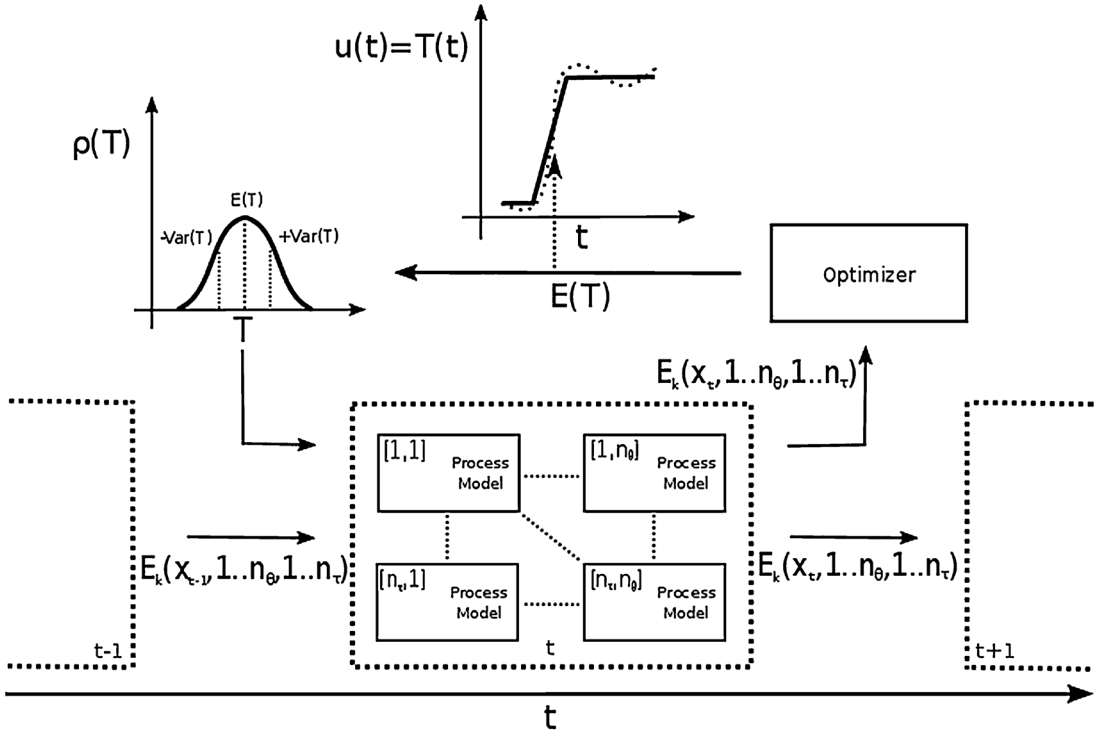


**Fig. 6.** Illustration of dynamic optimization approach for stochastic variables, see Level 3 optimization, $T$ – temperature, $t$ – (discrete) time, $x$ – arbitrary state variable, $n_\theta$ – amount of sigma points of uncertain model parameters, $n_\tau$ – amount of sigma points of non-uniform residence time.

**Table 4**
Confidence intervals of kinetic parameters and catalyst equilibrium.

| Variable | Eq. | $E_A$ (kJ/mol) | $k_0$ | Unit | $K_1$ (ml/mol) | $K_2$ (ml/mol) | $K_3$ (ml/mol) |
|---|---|---|---|---|---|---|---|
| $r_1$ | (1) | ±33.0% | ±13.9% | $\frac{ml^3}{g\ min\ mol^2}$ | ±355.0% | ±270.0% | ±1.0% |
| $r_2$ | (2) | ±29.0% | ±9.7% | $\frac{ml}{g\,min}$ | ±252.1% | ±21.0% | – |
| $r_3$ | (3) | ±26.0% | ±8.5% | $\frac{ml^2}{g\,min\,mol}$ | ±139.1% | ±97.2% | ±117.2% |
| $r_4$ | (4) | ±13.0% | ±6832.3% | $\frac{ml^2}{g\,min\,mol}$ | – | – | – |
| $r_5$ | (5) | ±408.0% | ±5.1% | $\frac{ml^3}{g\ min\ mol^2}$ | – | – | – |
| $r_6$ | (6) | – | ±10.9% | $\frac{ml^3}{g\ min\ mol^2}$ | – | – | – |
| $c_{cat}$ | (7) | – | – | – | ±84.1% | – | ±12.4% |

**Table 5**
Assumed confidence intervals for solubility constants and equilibrium constants.

| Variable | $\Delta G_2$ | $\Delta G_3$ | $H^0_{CO}$ | $H^0_{H_2}$ | $E_{A,H_{CO}}$ | $E_{A,H_{H_2}}$ |
|---|---|---|---|---|---|---|
| | ±10.0% | ±10.0% | ±10.0% | ±10.0% | ±10.0% | ±10.0% |

design optimization in each level are given in Tables 4 and 5. Main target of the robust design optimization on level 1 is the quantification of the impact of model parameter uncertainties on the predictive power of the performance.

To calculate the variances of the density functions of the uncertain model parameters the confidence intervals given in Tables 4 and 5 are taken as two times the standard deviation

$$\sigma^2_{\theta_i} = \left(\frac{E(\theta_i)\varepsilon_i}{2}\right)^2, \tag{21}$$

where $E(\theta_i)$ are the expected values from Tables 1–3 and $\varepsilon_i$ are the confidence intervals from Tables 4 and 5. Due to missing information of possible correlation all covariances are assumed to be zero leading to a diagonal covariance matrix $Cov(\boldsymbol{\theta})$ (Eq. (22)). Although it is possible to carry out the design steps assuming all of these parameters uncertain, it is not reasonable since only a few of them have an actual impact on the performance. Thus, a global sensitivity study is conducted by means of Sobol indices to identify the highly sensitive parameter uncertainties (Sobol', 2001). The rate constants of reaction 1 and 2, $k_{0,j}$, $j \in \{1, 2\}$„ and the non-zero constants in the catalyst equilibrium $K_{cat,1}$, $K_{cat,3}$ are considered as uncertain. The covariance matrix for these model parameters results in

$$Cov(\boldsymbol{\theta}) = \mathrm{diag}(\sigma^2_{\boldsymbol{\theta}}). \tag{22}$$

The arising probabilistic dynamic optimization problem in level 1 (PDOP 1) follows the form given in MDOP 3. Details can be found in Section S.I in the Supplementary Material.

### 2.7.2. Level 2 optimization

The time-based optimal control of level 1 can hypothetically be realized in a discontinuous reactor design, in which often a homogeneously mixed reaction zone can be assumed with certain degree of justification. In contrast, for designing a continuous reactor the optimal design with its control trajectories has to be transformed to a spatially distributed optimal design. The arising continuous flow and the distributed control is accompanied by non-idealities, e.g. due to flow field, diffusion phenomena or heat conduction and the corresponding axial and radial gradients. If those non-idealities are modeled in detail, e.g. as a 3D flow field, the complexity of the DAE system increases drastically and the convergence of the optimization might not be guaranteed anymore. Here we apply the probabilistic interpretation. In contrast to the uncertainties of the model parameters in the first level, the distribution of the variable of non-ideality does not describe its probability of occurrence. Instead the deviations itself are described, e.g. from ideal plug flow behavior in form of a steady-state segregated flow. Thus, radial mixing is neglected which leads to the idea of several parallel reactors without interaction regarding mixing. Starting from a predefined residence time distribution (RTD) at the end of the reactor, the moments of the RTD can be used to describe the non-ideal flow behavior. It has a special impact, since in this case the fluid elements traveling through the reactor are manipulated by the optimal control fluxes differently due to their different velocities. Hence another performance can be expected compared to the case of an ideal plug flow reactor. The arising probabilistic dynamic optimization problem in level 2 (PDOP 2) is derived from MDOP4 with $\vartheta$ being a distributed residence time (details see Section S.II in the Supplementary Material).

### 2.7.3. Level 3 optimization

In the third level of the design approach of Peschel et al. (2010) the technical approximation of the control profiles and design variables of level 2 is carried out. On this stage the consideration of imperfect approximation of the optimal control, e.g. due to systematic imprecision or a limited amount of actuators, or inaccuracies in the manufacturing of the optimal reactor can be included. In the following, we use the temperature control as an example for an imperfect design realization.

If the temperature control cannot be realized optimally, because heaters are not working precisely or the heat conductivity of the reactor material differs along the length, the temperature at each point in the reactor will deviate from the desired value in a certain degree. The inclusion of this type of randomness in the dynamic optimization differs from the two previously shown. Notably, the random variable is a control variable and thus dependent on the reaction coordinate. Its variations at each point of the reactor influence states and thereby the optimal control in all following points (Fig. 6). Therefore we apply MDOP 5 of our presented probabilistic design approach to derive the corresponding probabilistic design optimization problem on level 3 (PDOP 3). Details can be found in Section S.III of the Supplementary Material.

## 3. Results

Here we illustrate our probabilistic design approach and compare the results to the corresponding deterministic design. Therefore, we first solve the deterministic design optimization on level 1 of the EPF concept followed by three probabilistic design optimization steps that correspond to each of the three EPF levels including representative sources of uncertainties: model parameters (level 1), non-idealities of the flow field (level 2) and design approximation errors of the temperature control (level 3).

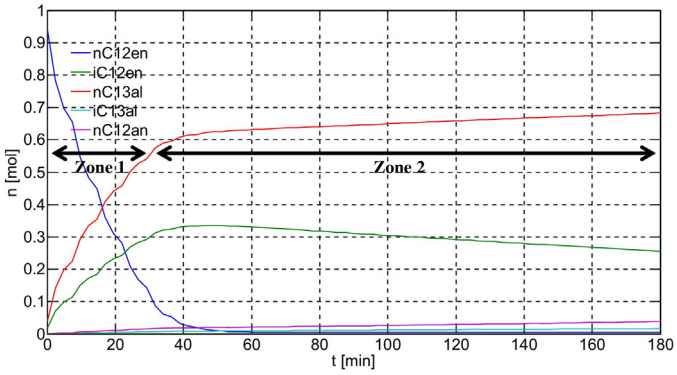


**Fig. 7.** Profiles of amounts of liquid substances resulting from the deterministic design optimization (DDOP) at $X = 0.995$.

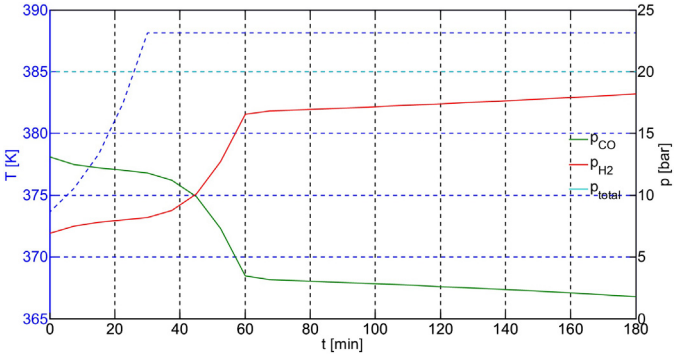


**Fig. 8.** Optimal control profiles from the deterministic design optimization (DDOP) at $X = 0.995$.

### 3.1. Deterministic design optimization

The problem formulation of the deterministic dynamic optimization (DDO) is given in the Supplementary Material in Section S.IV. Bounds and initial values for all DOP are listed in Table S2.

The design objective is to maximize the selectivity to the linear aldehyde tridecanal $S_{nC13al}$ The resulting optimal trend of the reactant concentrations over time are shown in Fig. 7. The corresponding optimal control of temperature and partial pressures are shown in Fig. 8. Due to changes in the reaction rate equations (Hentschel et al., 2015) the control differs slightly from those shown in Hentschel et al. (2014). As can be seen, the optimal reaction progress has two different reaction zones. In the first zone the temperature is slowly increased to the maximum temperature during excess of carbon monoxide in the gas phase. This control supports an ideal ratio of hydroformylation (red line) and isomerization (green line) in Fig. 7. In the second zone, where almost all reactant is converted, the temperature is kept at its maximum and the ratio of partial pressures shifts toward an excess of hydrogen. This leads to a backward-isomerization of the iso-dodecenes. The resulting 1-dodecene is then hydroformylated to additional aldehyde. The conditions in the second zone promote as well the formation of iso-aldehydes. Thus, the increase of selectivity to the *n*-aldehyde leads to a decreasing *n*/iso ratio. This is shown in Fig. 9, where the selectivity to the linear aldehyde and the ratio of linear to branched aldehydes is plotted over the conversion of the main reactant 1-dodecene. For a more comprehensive analysis of the reaction progress and a design of an optimal reactor embedded in an overall process the authors refers to the article of Hentschel et al. (2014).

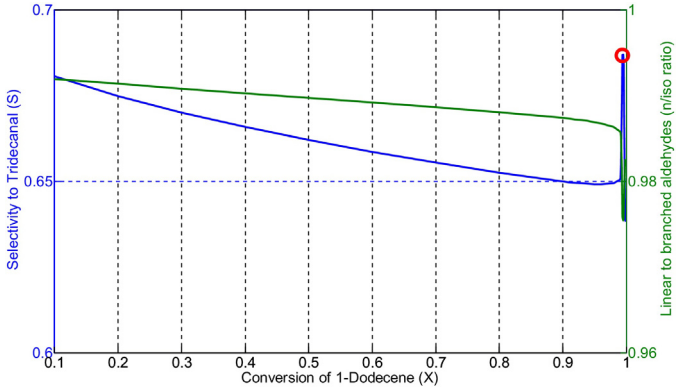


**Fig. 9.** Selectivity of the main product and *n*/iso ratio of the aldehydes over conversion in the deterministic design optimization. The optimal point of conversion is indicated by the red circle. (For interpretation of reference to color in this figure legend, the reader is referred to the web version of this article.)

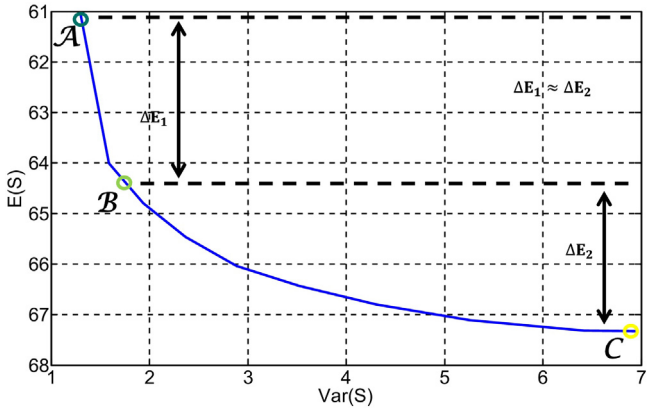


**Fig. 10.** Pareto front resulting from the robust design optimization in level 1 (PDOP 1) with $E_X(x) = 0.995$ illustrating the mean of the selectivity over its variance. Colored points (A, B, C) show the characteristic Pareto optimal design samples for further analysis in the grouped bar plots (see Figs. 14–16). (For interpretation of reference to color in this figure legend, the reader is referred to the web version of this article.)

### 3.2. Robust design optimization: Level 1

As stated in PDOP 1 (see Section S.I of Supplementary Material) the robust design optimization task in level 1 is to maximize the mean value of selectivity to the linear aldehyde (*n*-tridecanal) at minimal variance given four uncertain model parameters. The resulting Pareto set, calculated by the $\varepsilon$-constraint method, is shown in Fig. 10. The mean of the conversion is fixed at the optimal determined conversion $E_X(x) = 0.995$ (red circle in Fig. 9). As can be seen the Pareto optimality leads to loss in the expected selectivity for smaller variances and vice versa, see Fig. 10 dark green vs. yellow circles. Note that the yellow design point is close to the deterministic design case.

In Figs. 11–13 the optimal control profiles and optimal reaction times are shown for three Pareto optimal designs (see Fig. 10 colored circles (A, B, C)). For the three selected designs, the control profiles are qualitatively following the same behavior. In the first zone of the reaction progress the temperature is increased from lower to highest possible value and then stays almost constant until the end of the reaction time. The partial pressures are in a ratio of $p_{CO}/p_{H_2} = 2/1$ to 3/1 and shift to a ratio of ca. 1/3 at the end. These designs differ from the design without uncertainty (Fig. 8)

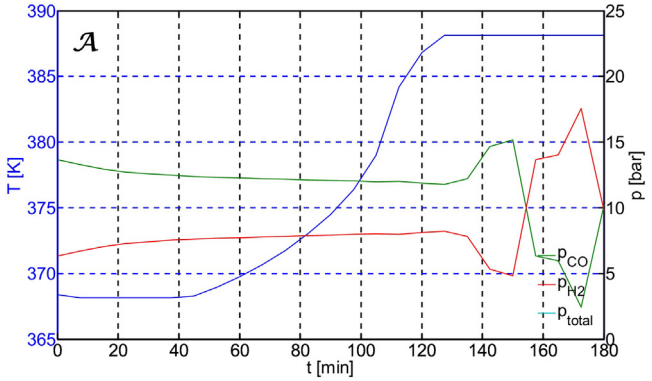


**Fig. 11.** Optimal control profiles resulting from the RDO (PDOP 1) with $E_X(x) = 0.995$ corresponding to the dark green point in Fig. 10.

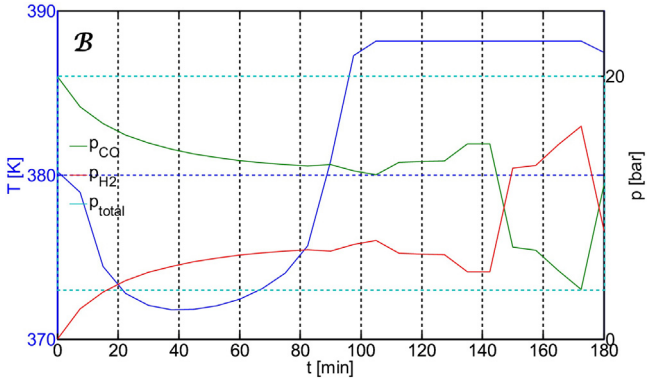


**Fig. 12.** Optimal control profiles resulting from the RDO (PDOP 1) with $E_X(x) = 0.995$ corresponding to the light green point in Fig. 10.

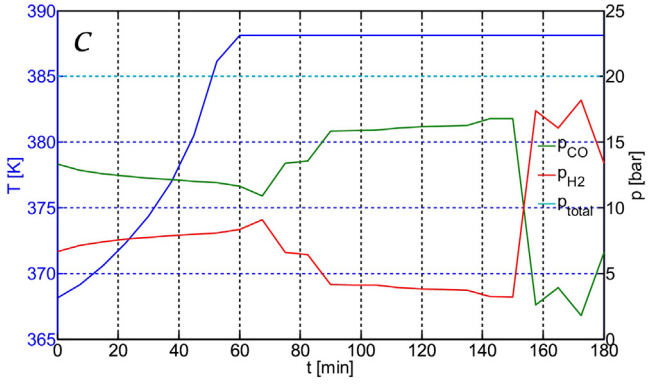


**Fig. 13.** Optimal control profiles resulting from the RDO (PDOP 1) with $E_X(x) = 0.995$ corresponding to the yellow point in Fig. 10.

only slightly regarding the time points of temperature and partial pressure ratio changes. But it is obvious that the more robust the process is designed the later the temperature shift is set and the smaller the partial pressure ratio is over most of the reaction progress. This can be explained by remembering the reaction zones in Fig. 7. The more robust the process should be the smaller the second reaction zone with higher temperature is chosen to keep more time for the first reaction zone since it is much more sensitive to the parameter uncertainties. Because the CO partial pressure

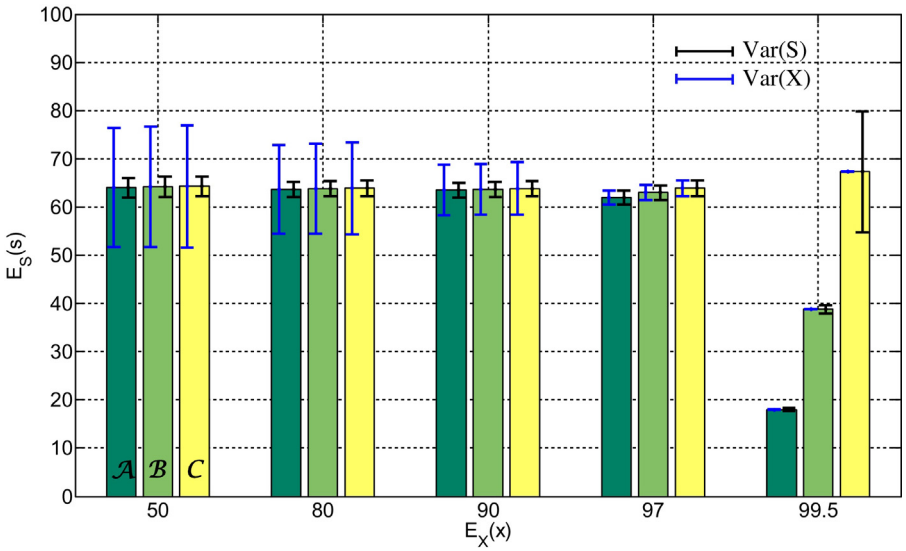


**Fig. 14.** Mean of the selectivity over mean of conversion resulting from PDOP 1 for several mean conversions, both in percent. Each group of bars is a Pareto set sampled at the colored points shown in Fig. 10. The bar colors match with the circle colors and indicate the chosen design points (A, B, C). The blue and black error bars show the corresponding variances of the conversion and the selectivity, respectively. (For interpretation of reference to color in this figure legend, the reader is referred to the web version of this article.)

is able to slow down the reaction rate by its inhibiting influence on the catalyst, the solver chooses to hold it high in case of uncertain parameters.

### 3.2.1. Comparison of the robust design optimization results for several conversions

So far the optimal operation point for conversion to achieve highest selectivity is considered to be at the same point as the results of the DDO revealed. To analyze whether the robustness of the performance can be further increased at other conversion points, we calculated Pareto sets for other mean conversions as well. In Fig. 14 we show mean values of the selectivity for five different mean conversion values in grouped bars. Each group consists of three bars corresponding to the three design points (A, B, C) in the Pareto set as indicated in Fig. 10. The black error bars show the variance of the selectivity at each point and the blue error bars the corresponding variances of the conversion.

For mean conversions of $E_X(x) = 0.5$, 0.8 and 0.9 the potential of the RDO to robustify the performance prediction and thus the reactor design is very low. Both, the variance of the selectivity and the variance of the conversion cannot be reduced significantly. For higher mean conversions of $E_X(x) = 0.97$ and 0.995 the influence of the design on the variance of the selectivity and conversion is higher. The variance of the conversion can be pushed to zero, but the variance of the selectivity is higher than for lower mean conversions. It can be reduced by expense of mean selectivity.

For the three lower conversions $E_X(x) \leq 0.9$ the optimal designs do not reach the second reaction zone (see Figs. 7 and 8). The reaction time in the first zone is rather short and therefore the variance of the conversion is higher, since not enough reaction time is available to reach the targeted conversion for all realizations of the parameters (represented by the set of sigma points). For the two higher conversions $E_X(x) \geq 0.97$ the reaction time is longer and the process provides enough time to reach the desired conversion for all parameter realizations. The variances of the conversion become very small. Furthermore the solver is forced to small conversion variances since conversions higher than 1 are not possible at all.

For the selectivity the mechanisms are different. Since the selectivity is much more depending on the reaction progress, deviating parameters have a higher impact on it. The increased variance of the selectivity at higher conversions results from the second reaction zone, where the shifts in temperature and partial pressures lead to additional formation of the linear aldehyde. This section of the reaction can either not be reached or is rather short for some parameter realizations. Finding an optimal control strategy that allows all parameter realizations to reach the second reaction section for optimal selectivity to the linear aldehyde is very difficult and leads to an optimal robust design prediction with strong decreased selectivity.

## 3.3. Robust design optimization: Level 2

To exemplify how non-idealities in the continuous reactor can be included in our probabilistic design procedure in addition to the model parameter uncertainties, the residence time is assumed non-ideal, i.e. with deviation from the desired plug-flow behavior (PDOP 2). The residence time $\tau$ is considered normally distributed, whereby its mean value corresponds to the case of ideal plug flow in level 1. The variance of the RTD is varied over a range to analyze its impact on the performance. For those varying RTDs the impact on the performance for a mean conversion of $H^0_{H2}$ is quantified exemplarily by calculating the corresponding Pareto sets. The results are depicted in Fig. 15, whereby the three bars in each bar group are again the aforementioned points in the corresponding Pareto sets (see Fig. 10).

The left case $\mathrm{STD}(\tau) = 0$ corresponds directly to the right case in Fig. 14. With increasing spread of the RTD the variance of the selectivity increases drastically by slightly decreasing mean selectivity. Note, that even a small deviation of the residence time decreases the width of the Pareto set drastically comparing to the case of plug flow ($\mathrm{STD}(\tau) = 0$). Conversion variance is almost not changing due to aforementioned reasons. For further design

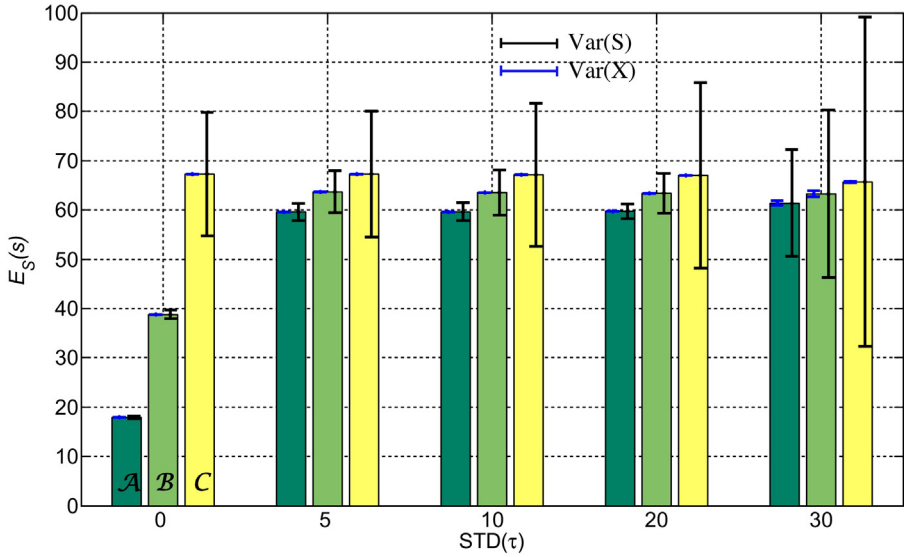


**Fig. 15.** Mean of the selectivity over the standard deviation (STD) of the residence time distribution, both in percent, resulting from PDOP 2. The blue and black error bars show the corresponding variances of the conversion and the selectivity, respectively. (For interpretation of reference to color in this figure legend, the reader is referred to the web version of this article.)

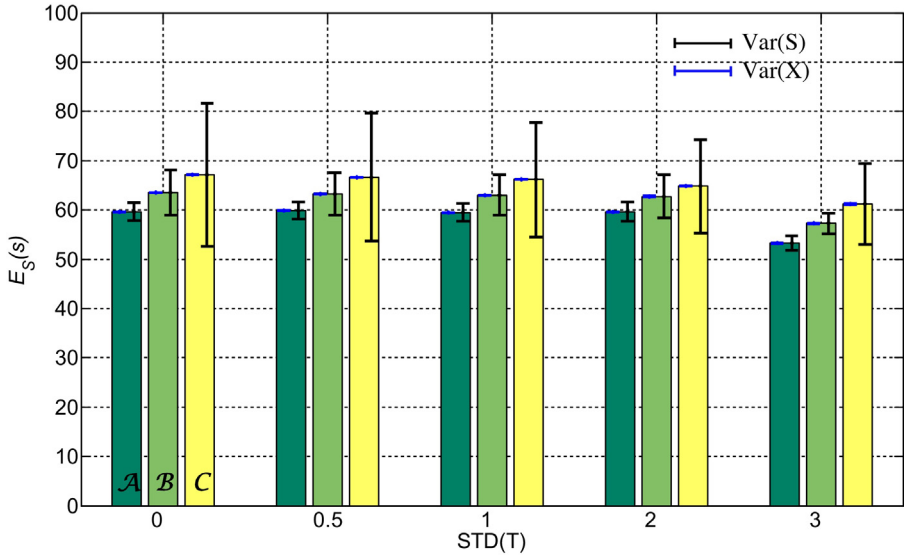


**Fig. 16.** Mean of the selectivity over the STD of the temperature STD($T$) in K resulting from PDOP 3. The blue and black error bars show the corresponding variances of the conversion and the selectivity, respectively. (For interpretation of reference to color in this figure legend, the reader is referred to the web version of this article.)

steps a STD($\tau$) = 10 is chosen to keep the variance of the selectivity small.

### 3.4. Robust design optimization: Level 3

At the end of the design procedure a technical approximation of the reactor design and its optimal control profiles is developed. In addition to the model parameter uncertainties in level 1 and the non-ideal RTD in level 2, an inaccurate realization of the temperature control profile is introduced in level 3. The impact on the performance and its predictive power is quantified and a robustification against all three types of uncertainties is carried out. In Section 2.3 it was shown how to include uncertainties that vary along the reaction time (see PDOP 3). The probabilistic dynamic optimization is carried out exemplarily for different STD of the optimal mean temperature control. The resulting Pareto sets are shown in form of grouped bars for the characteristic design points of the Pareto sets (see Fig. 10 for the characteristic design points). In Fig. 16 the results for temperature control STD of 0.5,. . .,3 K are depicted, whereby the left grouped bars are directly corresponding to the STD($\tau$) = 10 case in Fig. 15.

The grouped bars at STD($T$) = 0 correspond directly to the rightmost in Fig. 15. The temperature fluctuations have only a slight impact on the performance. With increasing temperature fluctuations the maximum expected selectivity decreases as expected. But interestingly this is accompanied by a decrease of its variance.

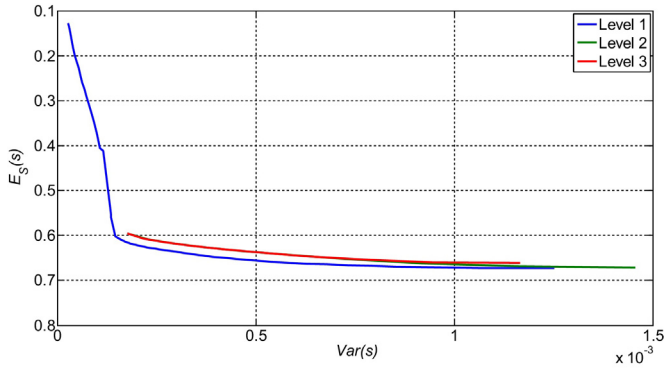


**Fig. 17.** Pareto sets for the three design levels. Level 1 with $E_X(x) = 0.995$ (blue line), level 2 with $E_X(x) = 0.995$ and STD($\tau$) = 10% (green line), level 3 with $E_X(x) = 0.995$ and STD($\tau$) = 10% and STD($T$) = 2 K (red line). (For interpretation of reference to color in this figure legend, the reader is referred to the web version of this article.)

The optimal solutions for the case of maximum mean selectivities (yellow bars, **C**) for higher fluctuations correspond to the slightly robustified solutions of the case without temperature fluctuations. The corresponding controls are almost similar as well. Only for very high fluctuations STD($T$) = 3 this does not suffice anymore and the mean selectivities have to be stronger reduced for compensation of the control fluctuations.

## 4. Discussion

In the previous section three different sources of randomness are included in an EPF based robust design optimization approach for chemical reactors: (i) model parameter uncertainties, (ii) non-idealities in reactor behavior and (iii) inaccuracies in the realization of the optimal design, which is related to deviations from the optimal control.

In level 1, deterministic and probabilistic designs are very similar, whereby the characteristic points of the design, namely the switches in temperature and partial pressure profiles, are shifted toward time points, which generate less sensitivity of the criterion to the model parameter uncertainties. Considering these results, it is promising to think about a reactor realization, which allows realizing nearly every point in the Pareto set, since the control trajectories of the designs with different robustness are quite similar. Such a flexible reactor design would be very beneficial for e.g. start-up processes or embedding in overall processes.

Already at this early stage of the design procedure a lot of additional information about the process is gained by use of the probabilistic approach. These information about the predictive power might also be used for an integrated overall process design. Since the design of subsequent separation units benefit more from a high predictive power than from a high expected value of the reactor outlet stream the possible enhancement of the overall process by applying the probabilistic design approach on it is promising. Since the focus of this article lies on the reactor unit design without its dependencies on other process units, these effects have not been analyzed. However, the probabilistic design approach allows doing so.

In Section 3.2 it was shown how the probabilistic design approach creates a framework to analyze impacts of parameter uncertainties on different performance measures and thereby identify the interdependencies of these measures. From this analysis it was concluded that model parameter uncertainties have very different impacts on the conversion and the selectivity. Here, new vistas are opened for the process designer. It is possible to choose a design with either conversion or selectivity, which is less sensitive to the model parameter uncertainties. This information is again even more valuable when additional information of the overall process requirements are available.

In level 2 of the design procedure non-idealities of the reactor behavior are introduced to the design approach. This was exemplified by the impact of a non-uniform residence time distribution, i.e. a deviation from ideal plug flow behavior. The mean of the RTD is the corresponding optimal residence time from the previous level, i.e. it was fixed to quantify only the impact of deviations from it. If the mean residence time is not to be fixed, the residence time itself can be included as a decision variable in the RDO. Moreover specific residence time distributions can be approximated with this method as well to investigate in particular their impact on the process. If they are not normally distributed one could use Gaussian Mixed Distributions (GMD) to introduce certain skewness. In case of non-segregated flow the non-uniform RTD has to be considered as a stochastic source of randomness and the approach of level 3 has to be applied.

In addition to the consideration of a RTD for describing a segregated steady-state flow field, non-idealities in the temperature field or pressure field can be included. This would lead to additional information about the required flow-field to avoid high radial temperature gradients and a high pressure drop. Latter could otherwise be compensated by change of the gas dosing strategy.

In level 3, the last step of the EPF design procedure, the optimal design of level 2 is approximated in a technical realization. A detailed description of the probabilistic design approach of level 3 is given in Section 2.7.3. It is clearly indicated that the presented probabilistic EPF approach enables the handling of stochastic variables that fluctuate along the reaction coordinate. The results in level 3 give an understanding of the impact of the design accuracy of a certain control variable. To use this knowledge for the design purpose additional information about the cost for each realization accuracy is necessary. Then one can find a trade-off between the cost for the accuracy of the control realization and the additional selectivity gained by it. In a similar way the accuracy of the design regarding partial pressure realization could be investigated.

Finally, Pareto sets for particular cases in level 1, 2 and 3 are compared in Fig. 17 to illustrate exemplarily the evolution of impacts of uncertainties/randomness on the performance and its predictive power.

It can be seen, that for every further considered source of uncertainty/randomness in the predicted design performance, the shape and position of the Pareto optimal solution sets are changing. The consideration of a non-uniform residence time distribution in level 2 results in a Pareto set which shows less robustification potential and higher uncertainty to realize the same performance as for the case with uniform RTD in level 1. The imperfect control realization in level 3 introduces an additional loss of performance especially in the area of high variance and high expected value of the selectivity.

Since almost every kind of uncertainty can be associated within the here presented classification, they can as well be included in the reactor design procedure. One can think of uncertain compositions of recycle streams, gradients in the radial temperature field, uncertain mass transfer rates, or catalyst degradation. Furthermore the presented approach is not limited to chemical reactors. The underlying DAE system can also describe other units in a chemical process, e.g. distillation columns, or other kind of processes, e.g. mechanical or fluid mechanical problems. In any case, to ultimately choose a design point the cost for realization of each design has to be known to find the best trade-off between cost and accuracy of the optimal design. The general procedure of analyzing the

impact of different kind of uncertainties/randomness on the design performance, as well for different performance measures, and the quantification of the impacts and the costs to reduce both leading to a profitable trade-off can be carried out for every kind of process.

A further smart property of our procedure is the possibility to reduce control burdens by choosing a more robust design which already compensates some uncertainty influences. If control burdens are included in the design procedure as additional objectives, a promising approach for simultaneous design and control of the reactor unit arises.

## 5. Conclusion

This article presents a new approach for probabilistic optimization by combining the EPF based reactor design approach of Peschel et al. (2010) with the sigma point method (Julier and Uhlmann, 1996). In contrast to existing work on robust design optimization based on sigma points, we developed a full probabilistic orthogonal collocation approach, i.e. random and stochastic variables are considered. Whereas the former one relates to stochastic variables that are independent on the reaction time (e.g. kinetic model parameters or initial conditions), the latter one describes stochasticity along the reaction time (e.g. fluctuating pressure or temperature control). As a reactor design example, we presented the hydroformylation of 1-dodecene in a thermomorphic solvent system consisting of n-decane and *N*,*N*-dimethylformamide. Applying our probabilistic EPF concept, we showed how to account for (i) model parameter uncertainties, (ii) non-idealities in the reactor behavior and (iii) inaccuracies in the realization of the optimal design. We further analyzed the benefits in view of the corresponding optimal deterministic design. Finally it was shown that: (i) a simultaneous analysis of the impact of randomness on more than one design criteria reveals their interdependencies and thus, opens new vistas for the process designer to choose a suitable reactor design; (ii) the presented method can be applied to roughly approximate the impacts of higher dimensional (2D, 3D) phenomena like flow fields on the performance and thus, reduces the optimization problem; and (iii) with this probabilistic approach influences of stochastic uncertainties can be quantified to find an optimal trade-off between realization costs and design performance.

## Acknowledgements

This work is part of the Collaborative Research Centre “Integrated Chemical Processes in Liquid Multiphase Systems” – InPROMPT. Financial support by the Deutsche Forschungs-Gemeinschaft (DFG) is gratefully acknowledged (TRR 63).

## Appendix A. Supplementary data

Supplementary data associated with this article can be found, in the online version, at http://dx.doi.org/10.1016/j.compchemeng.2016.06.008.

## References

Achenie, L.K.E., Biegler, L.T., 1990. A superstructure based approach to chemical reactor network synthesis. Comput. Chem. Eng. 14, 23–40.
Behr, A., Fängewisch, C., 2002. Temperature-dependent multicomponent solvent systems – an alternative concept for recycling homogeneous catalysts. Chem. Eng. Technol. 25, 143–147.
Behr, A., Henze, G., Johnen, L., Awungacha, C., 2008. Advances in thermomorphic liquid/liquid recycling of homogeneous transition metal catalysts. J. Mol. Catal. A: Chem. 285, 20–28.
Beyer, H.-G., Sendhoff, B., 2007. Robust optimization – a comprehensive survey. Comput. Methods Appl. Mech. Eng. 196, 3190–3218.
Bhaskar, V., Gupta, S.K., Ray, A.K., 2000. Applications of multiobjective optimization in chemical engineering. Rev. Chem. Eng. 16, 1–54.
Biegler, L.T., 1983. Solution of dynamic optimization problems by successive quadratic programming and orthogonal collocation.
Bohnen, H.-W., Cornils, B., 2002. Hydroformylation of alkenes: an industrial view of the status and importance. Adv. Catal. 47, 1–64.
Enevoldsen, I., Sørensen, J.D., 1994. Reliability-based optimization in structural engineering. Struct. Saf. 15, 169–196.
Flassig, R.J., Sundmacher, K., 2012. Optimal design of stimulus experiments for robust discrimination of biochemical reaction networks. Bioinformatics 28, 3089–3096.
Freund, H., Peschel, A., Sundmacher, K., 2011. Model-based reactor design based on the optimal reaction route. Chem. Ingen. Tech. 83, 420–426.
Freund, H., Sundmacher, K., 2008. Towards a methodology for the systematic analysis and design of efficient chemical processes: Part 1, From unit operations to elementary process functions. Chem. Eng. Process.: Process Intens. 47, 2051–2060.
Glasser, D., Crowe, C., Hildebrandt, D., 1987. A geometric approach to steady flow reactors: the attainable region and optimization in concentration space. Indus. Eng. Chem. Res. 26, 1803–1810.
Heine, T., Kawohl, M., King, R.,2006. Robust model predictive control using the unscented transformation. In: Computer Aided Control System Design, 2006 IEEE International Conference on Control Applications, 2006 IEEE International Symposium on Intelligent Control, 2006 IEEE. IEEE, pp. 224–230.
Hentschel, B., Kiedorf, G., Gerlach, M., Hamel, C., Seidel-Morgenstern, A., Freund, H., Sundmacher, K., 2015. Model-based identification and experimental validation of the optimal reaction route for the hydroformylation of 1-dodecene. Indus. Eng. Chem. Res.
Hentschel, B., Peschel, A., Freund, H., Sundmacher, K., 2014. Simultaneous design of the optimal reaction and process concept for multiphase systems. Chem. Eng. Sci. 115, 69–87.
Hillestad, M., 2010. Systematic staging in chemical reactor design. Chem. Eng. Sci. 65, 3301–3312.
Horn, F., 1964. Attainable regions in chemical reaction techniques. In: The Third European Symposium on Chemical Reaction Engineering, pp. 293–303.
Julier, S., Uhlmann, J., Durrant-Whyte, H.F., 2000. A new method for the nonlinear transformation of means and covariances in filters and estimators. IEEE Trans. Autom. Control 45, 477–482.
Julier, S.J., Uhlmann, J.K., 1996. A general method for approximating nonlinear transformations of probability distributions, Technical report. RRG, Department of Engineering Science, University of Oxford.
Kiedorf, G., Hoang, D., Müller, A., Jörke, A., Markert, J., Arellano-Garcia, H., Seidel-Morgenstern, A., Hamel, C., 2014. Kinetics of 1-dodecene hydroformylation in a thermomorphic solvent system using a rhodium-biphephos catalyst. Chem. Eng. Sci. 115, 31–48.
Kohlpaintner, C.W., Fischer, R.W., Cornils, B., 2001. Aqueous biphasic catalysis: Ruhrchemie/Rhône-Poulenc oxo process. Appl. Catal. A: Gen. 221, 219–225.
Kokossis, A.C., Floudas, C.A., 1991. Synthesis of isothermal reactor—separator—recycle systems. Chem. Eng. Sci. 46, 1361–1383.
Li, P., Arellano-Garcia, H., Wozny, G., 2008. Chance constrained programming approach to process optimization under uncertainty. Comput. Chem. Eng. 32, 25–45.
Markert, J., Brunsch, Y., Munkelt, T., Kiedorf, G., Behr, A., Hamel, C., Seidel-Morgenstern, A., 2013. Analysis of the reaction network for the Rh-catalyzed hydroformylation of 1-dodecene in a thermomorphic multicomponent solvent system. Appl. Catal. A: Gen. 462, 287–295.
Marler, R.T., Arora, J.S., 2004. Survey of multi-objective optimization methods for engineering. Struct. Multidiscip. Optim. 26, 369–395.
Mulvey, S.M., Vanderbei, R.J., 1995. Robust optimization of large-scale systems. Oper. Res. 43, 264.
Peschel, A., Freund, H., Sundmacher, K., 2010. Methodology for the design of optimal chemical reactors based on the concept of elementary process functions. Indus. Eng. Chem. Res. 49, 10535–10548.
Peschel, A., Karst, F., Freund, H., Sundmacher, K., 2011. Analysis and optimal design of an ethylene oxide reactor. Chem. Eng. Sci. 66, 6453–6469.
Rossner, N., Heine, T., King, R., 2010. Quality-by-design using a Gaussian mixture density approximation of biological uncertainties. Comput. Appl. Biotechnol., 7–12.
Schäfer, E., Brunsch, Y., Sadowski, G., Behr, A., 2012. Hydroformylation of 1-dodecene in the thermomorphic solvent system dimethylformamide/decane. Phase behavior–reaction performance–catalyst recycling. Indus. Eng. Chem. Res. 51, 10296–10306.
Schenkendorf, R., Kremling, A., Mangold, M., 2009. Optimal experimental design with the sigma point method. IET Syst. Biol. 3, 10–23.
Schuëller, G.I., Jensen, H., 2008. Computational methods in optimization considering uncertainties – an overview. Comput. Methods Appl. Mech. Eng. 198, 2–13.
Sobol', I.M., 2001. Global sensitivity indices for nonlinear mathematical models and their Monte Carlo estimates. Math. Comput. Simul. 55, 271–280.
Srinivasan, B., Bonvin, D., Visser, E., Palanki, S., 2003a. Dynamic optimization of batch processes: II. Role of measurements in handling uncertainty. Comp. Chem. Eng. 27, 27–44.

Srinivasan, B., Palanki, S., Bonvin, D., 2003b. Dynamic optimization of batch processes: I. Characterization of the nominal solution. Comput. Chem. Eng. 27, 1–26.
Telen, D., Vercammen, D., Logist, F., Van Impe, J., 2014. Robustifying optimal experiment design for nonlinear, dynamic (bio) chemical systems. Compu. Chem. Eng. 71, 415–425.
Wiebus, E., Cornils, B., 1994. Die großtechnische Oxosynthese mit immobilisiertem Katalysator. Chem. Ingen. Tech. 66, 916–923.
Xie, Z., Fang, J., Subramaniam, B., Maiti, S.K., Snavely, W., Tunge, J.A., 2013. Enhanced hydroformylation by carbon dioxide-expanded media with soluble Rh complexes in nanofiltration membrane reactors. AIChE J. 59, 4287–4296.